Methuen, London (1950).
Mason, E. A., and L. Monchick, "Heat Conductivity of Polyatomic and Polar Gases," *J. Chem. Phys.*, **36**, 1622 (1962).
Mason, E. A., A. P. Malinauskas, and R. B. Evans III, "Flow and Diffusion of Gases in Porous Media," *ibid.*, **46**, 3199 (1967).
Maxwell, J. C., "Illustrations of the Dynamical Theory of Gases," *Phil. Mag.*, **19**, 22 (1869). Also in The Scientific Papers of James Clerk Maxwell, Vol. I, p. 377, W. D. Niven, (ed.), Dover, New York (1958).
Miller, G. A., and R. L. Buice, "On the Knudsen Limiting Law of Thermal Transpiration," *J. Phys. Chem.*, **70**, 3874 (1966).
Reynolds, O., "On Certain Dimensional Properties of Matter in the Gaseous State," *Phil. Trans. Roy. Soc.* (London), **170**, 727 (1879).
Satterfield, C. N., Mass Transfer in Heterogeneous Catalysis, pp. 47-54, M.I.T. Press, Cambridge, Mass. (1970).
Weaver, J. A., and A. B. Metzner, "The Surface Transport of Adsorbed Molecules," *AIChE J.*, **12**, 655 (1966).

Manuscript received February 3, 1972; revision received March 30, 1972; communication accepted March 30, 1972.

Meniscus Vortexing in Free Coating

CHIE Y. LEE and JOHN A. TALLMADGE

Department of Chemical Engineering
Drexel University, Philadelphia, Pennsylvania 19104

The authors are interested in predicting meniscus flow effects. Although the need for describing curved menisci by two-dimensional flow fields has been recognized by Groenveld and Van Dortmund (1970) and others, a solution for a complete flow field in menisci has not been presented. Other aspects of this problem are referred to in the discussion.

Consider the case of free coating as shown in Figure 1A. Here a continuous flat sheet or belt is withdrawn upward at a constant velocity U_w from a liquid bath having a depth d and a width w. The thickness h of the adhering film will decrease from liquid level to a constant thickness h_0. Near the moving sheet, the streamlines are nearly parallel to the sheet and flow is upward because of the pumping action of the solid surface. Because a portion of liquid usually flows back down to the liquid bath, there is a stagnation point B at which the reverse flow occurs: a second stagnation point occurs at some point C. On the upper meniscus AB all the liquid flow is upward, and on the lower meniscus surface BC the liquid flow is downward. The case considered here is steady flow, where the same mass flux Q of liquid withdrawn by coating is added to the right corner of bath. This feed flow maintains the liquid level. Since flow is downward near the liquid inlet, an eddy is created in the lower right corner of Figure 1A and a vortex is usually created in the bath below BC.

The main purposes of this paper are to predict the vortex and stagnation points in free coating and to confirm the theory with data.

THEORY

Neglecting edge effects, the coating process can be described by a steady state, two-dimensional model in rectangular coordinates. The relevant differential equations are those of continuity and motion for the well-known Navier-Stokes fluid, which has constant density and constant viscosity. For the x direction vertically upward, these equations reduce to the following expression for velocity components $u(x, y)$ and $v(x, y)$.

$$\frac{\partial u}{\partial x} + \frac{\partial v}{\partial y} = 0 \tag{1}$$

$$\rho\left[u\frac{\partial u}{\partial x} + v\frac{\partial u}{\partial y}\right] = \mu\left[\frac{\partial^2 u}{\partial x^2} + \frac{\partial^2 u}{\partial y^2}\right] - \frac{\partial P}{\partial x} - \rho g \tag{2}$$

$$\rho\left[u\frac{\partial v}{\partial x} + v\frac{\partial v}{\partial y}\right] = \mu\left[\frac{\partial^2 v}{\partial x^2} + \frac{\partial^2 v}{\partial y^2}\right] - \frac{\partial P}{\partial y} \tag{3}$$

Eleven boundary conditions are applicable. Six of the BC's are no slip of u or v at each of three solid boundaries (continuity of velocity). BC 7 and 8 are known velocities for the constant thickness region at a distant "a" far above the liquid level; these velocity profiles are

$$v = 0,\ u = \frac{h_0^2 \rho g}{2\mu}\left[\left(\frac{y}{h_0}\right)^2 - 2\left(\frac{y}{h_0}\right)\right] U_w \tag{4, 5}$$

The remaining three BC's involve the gas-liquid interface $h(x)$. Here they are taken as BC 9 continuity of net flow across any horizontal cross section of the film, BC 10 negligible tangential stress, and BC 11 meniscus profiles $h(x)$ obtained experimentally.

For convenience in solution, the stream function ψ^0 and the vorticity ω^0 are introduced in the standard way, $u = \partial\psi^0/dy$, $v = -\partial\psi^0/\partial x$, and Equation (6) for ω^0. Thus Equations (1) to (3) may be replaced by

$$-\omega^0 \equiv \frac{\partial u}{\partial y} - \frac{\partial v}{\partial x} = \frac{\partial^2 \psi^0}{\partial y^2} + \frac{\partial^2 \psi^0}{\partial x^2} \tag{6}$$

$$\left[\frac{\partial \psi^0}{\partial y}\frac{\partial \omega^0}{\partial x} - \frac{\partial \psi^0}{\partial x}\frac{\partial \omega^0}{\partial y}\right] = \frac{\mu}{\rho}\left[\frac{\partial^2 \omega^0}{\partial y^2} + \frac{\partial^2 \omega^0}{\partial x^2}\right] \tag{7}$$

Equation (6) follows from the definitions of ψ^0 and ω^0. The continuity Equation (1) is automatically satisfied by the stream function ψ^0. The motion Equations (2) and (3) combine to form Equation (7) by elimination of the pressure terms.

It is convenient to make Equations (6) and (7) non-

Correspondence concerning this communication should be addressed to J. A. Tallmadge. C. Y. Lee is at Pennwalt Corp.; Warminster, Pennsylvania.

dimensional for the purpose of numerical solution and analysis. Using U_w and $h_c = (\mu U_W/\rho g)^{1/2}$ as characteristic speed and length, Equations (6) and (7) were multiplied by h_c/U_w and $(h_c/U_w)^2$ respectively to obtain

$$-\omega = \frac{\partial^2\psi}{\partial Y^2} + \frac{\partial\psi}{\partial X^2} \tag{8}$$

$$\left[\frac{\partial\psi}{\partial Y}\frac{\partial\omega}{\partial X} - \frac{\partial\psi}{\partial X}\frac{\partial\omega}{\partial Y}\right] = \frac{1}{Re}\left(\frac{\partial^2\omega}{\partial Y^2} + \frac{\partial^2\omega}{\partial X^2}\right) \tag{9}$$

Taking $\psi = 0$ along the three solid walls (one sheet wall and two bath walls), the eleven boundary conditions for Equations (8) and (9) are given for $\psi(X, Y)$ and $\omega(X, Y)$ as follows. BC's one to three involve no slip at the walls:

$$\psi(X, W) = \psi(0, Y) = \psi(X, 0) = 0 \quad (10, 11, 12)$$

The other three no slip conditions (BC's 4 to 6) were written first in terms of $\partial\psi/\partial Y = 0$ at $X = 0$ and $\partial\psi/\partial X = 0$ at $Y = 0, W$ but used in the vorticity form given by

$$\omega = -\frac{\partial^2\psi}{\partial X^2} \text{ at } X = 0; \quad \omega = -\frac{\partial^2\psi}{\partial Y^2} \text{ at } Y = 0, W. \tag{13, 14, 15}$$

The constant-region, boundary conditions 7 and 8 involved $\partial\psi/\partial X = 0$ and $\psi = \psi_0(T_0)$ where $T_0 \equiv h_0/h_c$, or

$$\psi = Y + (Y^2/6)(Y - 3T_0) \text{ at } X \geq (A + D) \tag{16}$$

$$\omega = -\frac{\partial^2\psi}{\partial Y^2} \text{ at } X \geq (A + D) \tag{17}$$

Interfacial boundary conditions 9, 10, and 11 for flux, tangential stress, and profiles are given at $Y = H$ by

$$\psi = Q = \int_0^Y \frac{u dY}{U_w} = Q_0 = T_0[1 - (T_0^2/3)] \tag{18}$$

$$\omega = 2V_s C \tag{19}$$

$$H = H(X) \text{ from data} \tag{20}$$

The interfacial curvature C is determined from the meniscus profile $H(X)$, given by Equation (20). The vorticity Equation (19) was derived as follows: Let s be the length along a stream line and n the length normal to it. The velocity vector is specified by its magnitude V and the inclination θ with respect to the x axis. Using the continuum approach, Emmons (1958) has shown that the vorticity along a streamline in steady two-dimensional flow is given by

$$\omega^0 = -\frac{\partial V}{\partial n} + V\frac{\partial\theta}{\partial s} \tag{21}$$

Emmons (1958) has also shown that the tangential strain e_{ns} along a streamline in steady two-dimensional flow is given by

$$e_{ns} = \frac{\partial V}{\partial n} + \frac{\partial\theta}{\partial s}(V) \tag{22}$$

At the gas-liquid interface with negligible gas phase drag, the tangential stress and strain is taken as zero. Thus Equation (22) indicates that

$$\frac{\partial V}{\partial n} = -V\frac{\partial\theta}{\partial s} \tag{23}$$

Substituting Equation (23) into Equation (21) leads to the vorticity along the gas interface, which is $\omega^0 = 2V(\partial\theta/\partial s)$. Here $\partial\theta/\partial s$ is equal to the curvature, so that $\omega^0 = 2Vc$, which is the dimensional form of Equation (19).

NUMERICAL RESULT

Equations (8) and (9) were solved numerically by iteration for several conditions. One of the cases is given in Figure 1B in terms of predicted streamlines. As shown in Figure 1B, the theory predicts two stagnation points, marked by circles at S_1 and S_2, and a vortex cell structure. Furthermore, the vortex cell is bounded by a streamline which has a value of the stream function ψ equal to the interfacial value, $\psi_0 = Q_0$, as given by Equation (18). The location of the upper stagnation point agrees approximately with that predicted by Lee and Tallmadge (1972A) using a one-dimensional model; the predicted location is given in terms of the thickness h_s by

$$\frac{h_s}{h_0} = 3 - \left[\frac{h_0^2\rho g}{\mu U_w}\right] = 3 - T_0^2 \tag{24}$$

EXPERIMENT

The conditions for the theory in Figure 1B were chosen for direct comparison with an experimentally obtained condition. Using a continuous belt device described by Soroka and Tallmadge (1971), a viscous fluid and a sizable speed were chosen to provide a large Ca, a large meniscus deformation and a thick film h_0. The withdrawal speed was 143 mm/s and the fluid properties of the 99% glycerine-water solution at 25.5°C were a viscosity of 0.86 N-s/m² (8.6 poise), surface

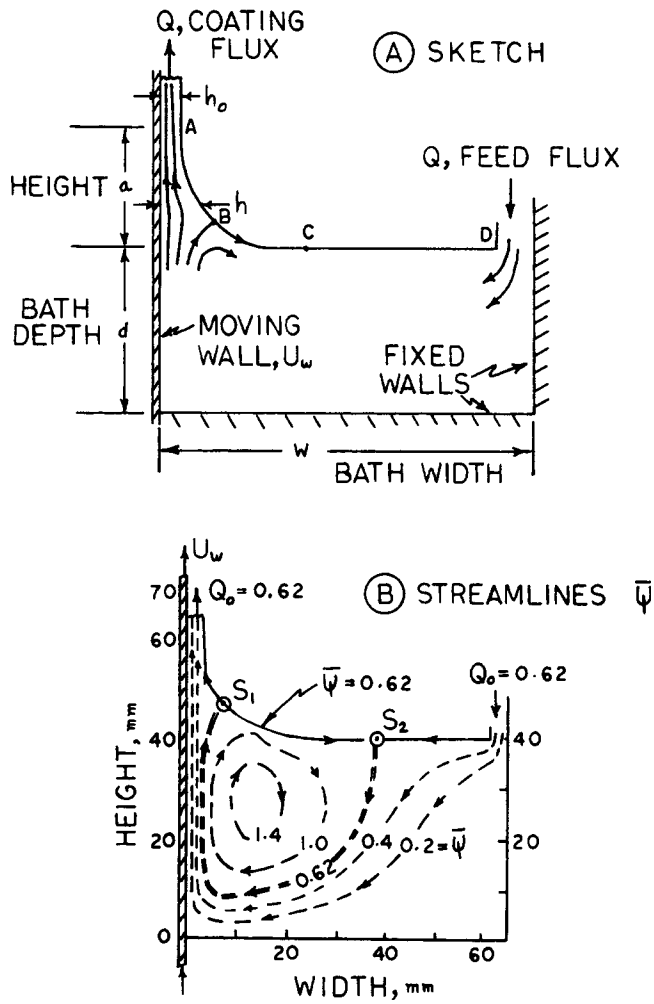

Fig. 1. Free coating in a finite bath. Part A shows sketch of free coating. Part B shows the $\bar{\psi}$ streamlines predicted by theory for the conditions of Run 901G ($Ca = 2.1$, $Re = 0.7$, and bath size of 40 by 65 mm).

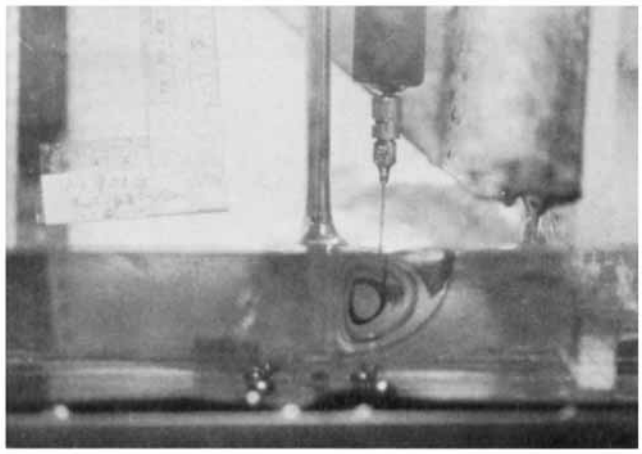

Fig. 2. Photographic data. Part A shows the vortex in Run 901G after 30 s of dye injection. Part B shows the vortex in the same run after 300 s of dye injection. Each photograph is a side view of belt coating by vertical withdrawal in Run 901G (143 mm/s and a bath size of 40 by 65 mm). The fluid is glycerine having a viscosity of 0.86 N-s/m², so the F_p number is about 2.1.

tension of 0.0616 N/m, and a density of 1260 kg/m³. At these conditions the capillary number is about 2.1 and the Reynolds number is about 0.7; the resultant thickness T_0 was found to be 0.75 and the flux ($Q = \psi_0$) was 0.62.

A bath depth of 40 mm was selected as a compromise between a large bath size (preferred for ease in experiment) and a small bath size (preferred for theory in order to minimize computer time and storage). The bath width of 65 mm was chosen arbitrarily to be somewhat larger than the depth. The bath depth was adjusted by varying the amount of fluid in the container and the bath width was adjusted by inserting a plate inside the container. A new container (No. 6) was used to allow better photographs. The container was made of 8 mm thick, clear plexiglas and was 250 by 200 mm in horizontal cross section. Here 250 mm was perpendicular to the belt surface (composed of 75 mm on the wiped back side and 175 mm on the free coating side) and 200 mm was parallel to the belt surface (with each distance between the belt edge and the side wall of about 70 mm). The new design used uninterrupted side walls.

A dye injection technique was developed to trace stream lines and to locate the vortex cell, using blue ink diluted with glycerine to obtain the dye. A 20 ml syringe with a 0.5 mm I.D. needle was used for injecting the colored glycerine into the white glycerine of the liquid bath. Dye was injected into various positions within the vortex region and photographed over a period of several minutes.

The photographs in Figure 2 were obtained using black and white ASA 400 film at f3 and 1/250 second. The 35 mm Nikon camera was placed at a distance of 210 mm from the side wall of the liquid container. Thus Figure 2 presents an edge view of the belt with a free coating side on the right and the wiped back side on the left. The view is also through 200 mm of the liquid. Flow around the sides was negligible.

COMPARISON WITH DATA

The photographs of Figure 2 confirm the existence of a vortex cell and of two stagnation points, as predicted by theory in Figure 1B. Figure 2 also provides qualitative agreement between theory and data in the size of the vortex cell (defined by the $\psi_v = \psi_0$ streamline) and in the location of the stagnation points and other streamlines. In addition, the photographs show that two-dimensional, free coating flow is obtainable in the laboratory. Color cinematography with a super-8, Minolta camera showed that aluminum foil, when placed in the vortex, was trapped and did not leave the cell. This foil result also confirmed that the ψ_v streamline is equivalent to a physical barrier to flow.

DISCUSSION OF THEORY

Confirmation of the theoretical approach by data suggests that the theory can be used to study the effect of several parameters such as bath size, feed location, *Ca* and *Re*. The theoretical approach is a new application of the two-dimensional equations and has potential use in prediction of meniscus flow fields in other geometries, such as in Kayser and Berg (1971). The approach may also provide a basis for predicting more accurate meniscus profiles than those by one-dimensional models, such as Lee and Tallmadge (1972A), and for predicting the onset of film nonuniformities. The agreement of theory with data encourages work on reducing computer time by improving the numerical scheme. In summary, this theory predicts the flow field in the curved meniscus case of free coating (Lee and Tallmadge, 1972B).

ACKNOWLEDGMENT

This work was supported in part by the Eastman Kodak Company.

NOTATION

a = height of meniscus, mm
A = height of meniscus, dimensionless, a/h_c
c = interface curvature, mm^{-1}
Ca = Capillary number, $\mu U_w/\sigma$
d = bath depth, mm
D = bath depth, dimensionless, d/h_c
h = meniscus thickness at any point, mm
h_0 = film thickness in constant thickness region, mm
h_c = characteristic length, $(\mu U_w/\rho g)^{1/2}$; mm
F_p = fluid property number, $\mu(g/\rho\sigma^3)^{1/4}$
P = pressure, N/m²
Q = mass flow rate per unit width, dimensionless, Equation (18)
Re = Reynolds number, $h_c U_w \rho/\mu$
T_0 = thickness, h_0/h_c
U_w = withdrawal speed of belt, mm/sec
u, v = velocity components in x and y directions, mm/sec
V_s = surface velocity, dimensionless
x, y = vertical and horizontal coordinate, mm
w = bath width, mm
W = bath width, dimensionless, w/h_c
ψ = stream function, dimensionless
ω = vorticity, dimensionless

LITERATURE CITED

Emmons, J. B., Fundamentals of Gas Dynamics, p. 57 and 62, Princeton Univ. Press, N. J. (1958).

Groenveld, P., and R. A. Van Dortmond, "Shape of the Air Interface During the Formation of Viscous Liquid Films by Withdrawal," *Chem. Eng. Sci.*, **25**, 1571 (1970).

Kayser, W. V., and J. C. Berg, "Spontaneous Convection in the Vicinity of Liquid Meniscuses," *Ind. Eng. Chem. Fundamental*, **10**, 526 (1971).

Lee, C. Y., and J. A. Tallmadge, "Deformation of Meniscus Profiles in Free Coating," 46th Nat. Collid Sym., Univ. of Mass., Amherst (1972A).

———., "Meniscus Vortexing in Free Coating," presented at National Am. Inst. Chem. Engrs. Mtg., Minneapolis, Minn. (1972B).

Soroka, A. J., and J. A. Tallmadge, "Test of the Inertial Theory for Plate Withdrawal," *AIChE J.*, **17**, 505 (1971).

Manuscript received March 17, 1972; revision received May 3, 1972; communication accepted May 3, 1972.